Supercond. Sci. Technol. **13** (2000) L25–L30. Printed in the UK PII: S0953-2048(00)13709-1

RAPID COMMUNICATION

Percolation modelling for highly aligned polycrystalline superconducting tapes

N A Rutter, B A Glowacki and J E Evetts

Department of Materials Science and Metallurgy, University of Cambridge, Pembroke Street, Cambridge CB2 3QZ, UK
and
IRC in Superconductivity, Madingley Road, Cambridge CB3 0HE, UK

Received 4 May 2000

Abstract. Surface and bulk texture measurements have been carried out on highly aligned NiFe tapes, suitable for use as coated conductor substrates. Data from small-area electron backscatter diffraction measurements are compared with those from bulk x-ray analysis in the development of a two-dimensional percolation model, and the two are shown to give very similar results. No evidence of grain-to-grain correlation is found. The model is then developed to assess how the properties of a superconducting layer grown epitaxially on buffered tapes will depend on parameters such as sample size, grain size and the extent of grain alignment.

1. Introduction

Coated conductors consist of a network of superconducting grains with good crystallographic alignment. Current flow is dependent upon the (low angle) grain boundaries which limit the critical current of a sample. The dependence of critical current density (J_c) on grain boundary angle in YBCO has been studied extensively in bicrystal samples and has been shown to decrease exponentially with the misorientation angle (θ) for $\theta > 10^\circ$ [1, 2]. Low-angle grain boundaries are structurally very different from high-angle grain boundaries, consisting of dislocation arrays, rather than regions of complete structural disorder. These two regimes of boundary do, however, appear to have similar effects in limiting the critical current [2]. Various data, from measurements on three distinct types of grain boundary, are shown in figure 1. Although there is a significant spread in the data, an exponential decrease of J_c with increasing angle gives a reasonable fit. Also, it is interesting to note that the type of boundary does not appear to be highly significant in determining its effect on current flow.

Because of this decrease of J_c with boundary angle, it is essential to produce a highly aligned superconducting layer when developing a coated conductor. In the process known as RABiTS [3], this depends on having a highly oriented metallic substrate, usually Ni or a Ni-based alloy. It has been shown by transmission electron microscopy (TEM), magneto-optical imaging (MOI) and electron backscatter diffraction (EBSD) that grain boundaries in the substrate layer are transferred through the buffer layers to the superconducting film [4, 5]. Hence the buffer layers and superconductors grow epitaxially, their textures being determined by that of the substrate. This does not, however, mean that all layers will show exactly the same extent of crystallographic alignment. For example, YSZ buffer layers deposited on CeO_2 on NiFe tapes can have x-ray FWHMs of 3° compared with about 6° in the substrate. Other techniques may produce buffer layer textures that are significantly poorer. There can also be significant differences in the extent of alignment in the superconducting layer. When YSZ is the uppermost buffer layer, there is a significant improvement in the out-of-plane (c-axis) alignment of YBCO, due to the low

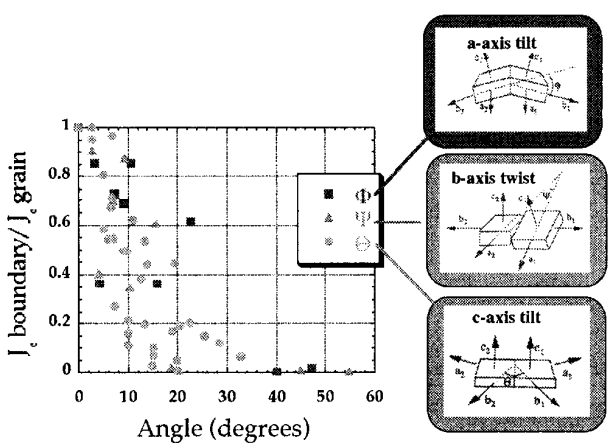

Figure 1. The dependence of the grain boundary critical current on misorientation angle for three possible boundary types.

(001) surface energy and anisotropic growth mode, favouring the alignment of the YBCO c-axis perpendicular to the film surface [6]. When a CeO_2 cap layer is used, the lattice match between superconductor and buffer is much better. Epitaxial growth is now more favourable and the out-of-plane texture improvement is no longer evident [7].

The percolative properties of such a grain structure are obviously important in determining the critical current of a coated conductor consisting of a network of low-angle grain boundaries. It is useful to study the extent to which a sample is connected when a given boundary angle is tolerated. For example, a simple model might assume that current can flow only through boundaries with misorientation angles less than, say, 5°. It would then be useful to assess parameters such as the probability of percolation through a sample, the extent of the connection region, and the size of the smallest restricting region of flow between the sample ends.

The critical current of a sample may be assessed using a limiting interface model. By determining the weakest interface (consisting of grain boundaries) perpendicular to the current flow direction, it is possible to calculate the J_c of a modelled sample. This type of model has been used previously to study the effect of in-plane texture of c-axis films [8], and the shape of I–V characteristics [9, 10].

2. Experiment

2.1. Experimental procedure

Electron backscatter diffraction measurements were carried out on small lengths of NiFe tape using the OPAL system [11]. The standard maps are based on a 64×48 square array of pixels covering an area of approximately 200×150 μm^2. Larger area maps may be produced from a montage of several individual sets of measurements. Note that the average (linear) grain size of the NiFe tapes used is approximately 30 μm.

X-ray measurements were made using a Phillips PW1710 vertical diffractometer and X'PERT 4-axis texture goniometer. Rocking curves (in both rolling and transverse directions) and phi scans were measured for five NiFe tape samples in order to assess the extent of crystallographic alignment of the material.

2.2. Modelling

It is possible to represent a two-dimensional grain structure of identical regular polygons with either a square or a hexagonal array. The crucial difference between the two, from a percolation viewpoint, is the number of neighbours of each grain: four and six respectively. The square array is slightly more straightforward to model and has been used extensively in percolation modelling [8, 12]. However, the hexagonal array is a more realistic simulation of a real grain structure (despite still being a large oversimplification) and is therefore used in this model. A 'sample' of length l and width w is defined by a two-dimensional array of R rows and C columns as indicated in figure 2.

The crystallographic orientation of any grain in a sample may be characterized by the use of three Euler angles which define a rotation matrix [13]. The rotation matrices of two

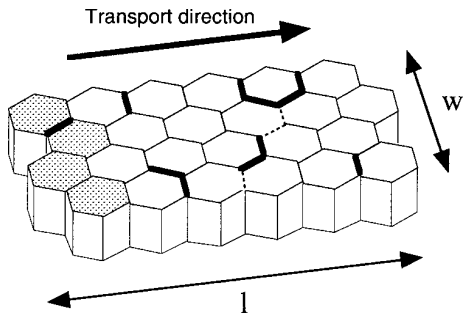

Figure 2. The two-dimensional hexagonal array of grains consists of R rows and C columns forming a sample of width w and length l (note $R = 4$, $C = 6$). In the model, current is injected at one end, into the grains on the left (shaded).

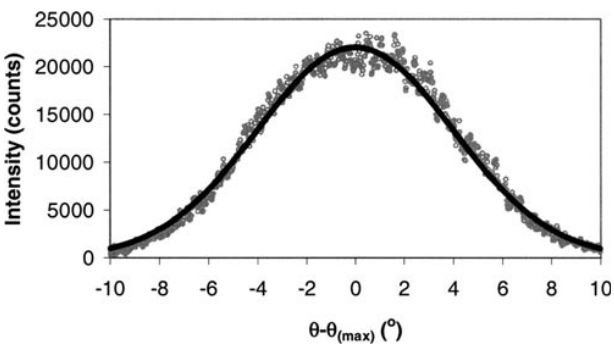

Figure 3. X-ray rocking curve in the transverse direction of the NiFe tape (open circles) fitted to a binomial distribution (full curve).

grains may then be combined to calculate their relative angle of misorientation. Using two sets of three Euler angles, the misorientation of two 'grains' in the modelled sample may be calculated [14]. The Euler angles assigned to each grain are based on a distribution which reflects the crystallographic texture of the material. Figure 3 shows an x-ray rocking curve (open circles), to which a Gaussian distribution is fitted. This type of distribution, based on the FWHM of rocking curves and phi scans, is used throughout in order to assign the three Euler angles to each grain. Having done this, it is then possible to calculate the misorientation of a grain from each of its neighbours and therefore to assign a misorientation angle to each grain boundary in the sample.

When a given angle criterion is imposed, the grain boundaries become either 'open' or 'closed' depending on whether their misorientation is smaller or greater than the threshold. Several percolation parameters may then be assessed by studying a large number of modelled samples. The first of these is the percolation probability, an indication of the likelihood that an open path exists from one end of the sample to the other. If such a path does exist it is useful to identify what fraction of the sample width is open, i.e. whether there is effectively 'free flow' across the whole width of the sample, or whether percolation through the tape is restricted within a few grains. Another parameter, which can be assessed regardless of the existence of a path, is the fraction of the total number of grains which it is possible to percolate into (through open boundaries) from one end of the sample. As an example of these parameters, consider again

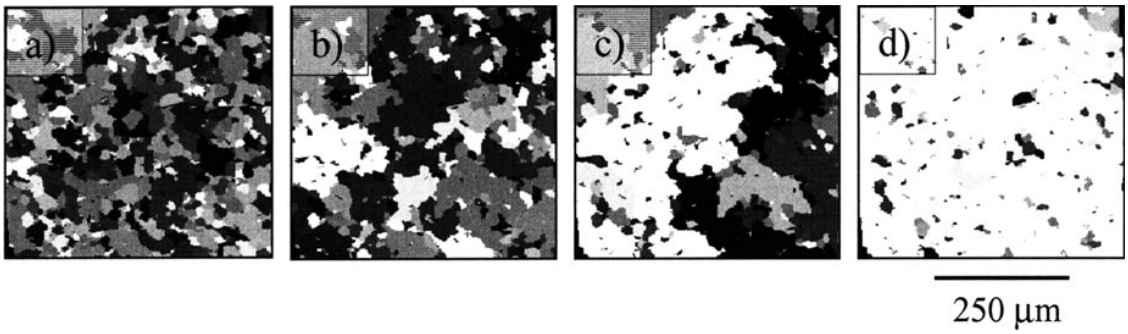

Figure 4. Maps showing percolating regions in an area of the NiFe tape with thresholds of (a) 2°, (b) 4°, (c) 5° and (d) 6°.

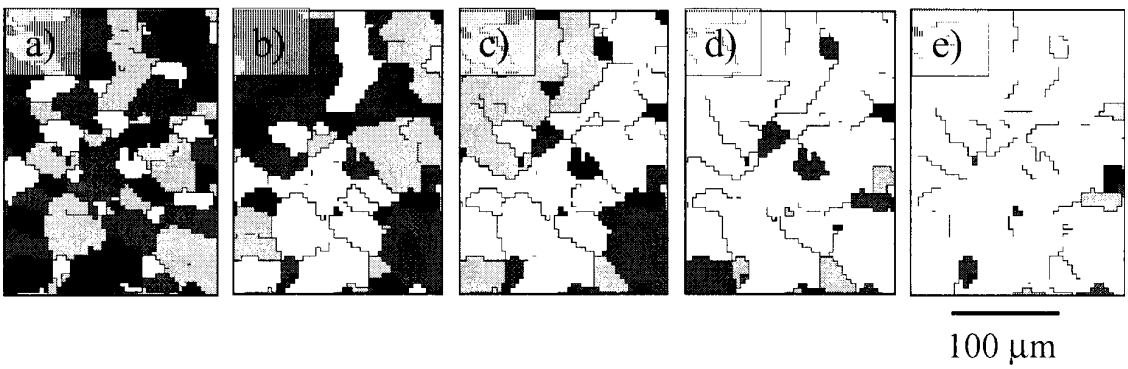

Figure 5. More detailed percolation maps, including all boundaries with misorientations greater than the threshold. Threshold values are (a) 2°, (b) 4°, (c) 5°, (d) 6° and (e) 8°.

figure 2, which represents a possible modelled sample. One injects current into the shaded cells on the left in order for it to percolate into the rest of the sample in the direction shown. All boundaries are considered to be open, except those marked with the heavy line. Percolation to the other side can occur, hence in this example the percolation 'probability' is 1. In the region marked with a dotted line, only 3/7 (43%) of the sample width is open and of the 20 cells which make up the sample, 19 (95%) can be reached. The results obtained in this way have been compared with measurements taken from the EBSD maps in order to assess the suitability of the hexagonal grain model, before using it as a basis on which to model the current-carrying capacity of granular samples.

3. Results and discussion

3.1. EBSD measurements

EBSD measurements were carried out on a region of the NiFe tape approximately $400 \times 400\ \mu m^2$ in area. The maps in figure 4 shows regions which are connected by grain boundaries that have misorientation values less than the tolerance angle indicated. The maps demonstrate that there is a critical angle of around 5° at which percolation through the sample becomes possible. Figure 4(d) demonstrates that over 90% of the sample is connected when 6° boundaries are tolerated. This would seem to indicate that transport along the tape across boundaries less than 6° would be relatively unobstructed, although figure 5 demonstrates that this is not the case. Figure 5 shows, in more detail, measurements made on a smaller area of the sample and includes the closed boundaries as well as the percolating regions. The first thing to note

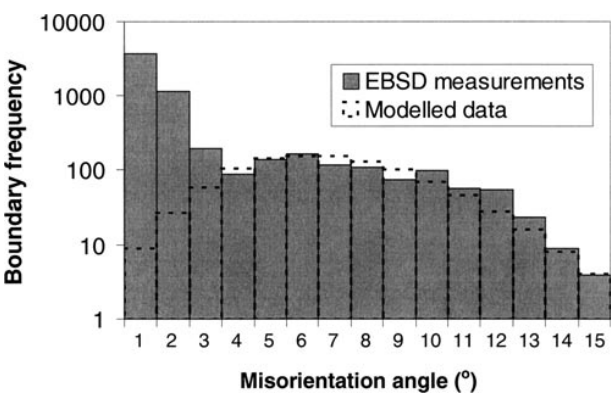

Figure 6. Histogram showing grain boundary angle distribution in the region shown in figure 5 (shaded bars) and predicted by a bulk texture model (dotted lines).

is that measurements on this scale are still representative with percolation still occurring at a threshold of around 5°. Figure 5(d) demonstrates that, despite the fact that a large proportion of the sample is connected (about 90%), it is necessary to pass through a constriction which is as small as 10% of the sample width, when traversing the tape from top to bottom. It can be seen in figure 5(e) that there are also a large number of boundaries with greater than 8° misorientation present, which may severely restrict flow through the sample.

3.2. Grain-to-grain correlation

The pixel-to-pixel misorientation distribution is shown in figure 6 (shaded bars). Its form is consistent with that usually

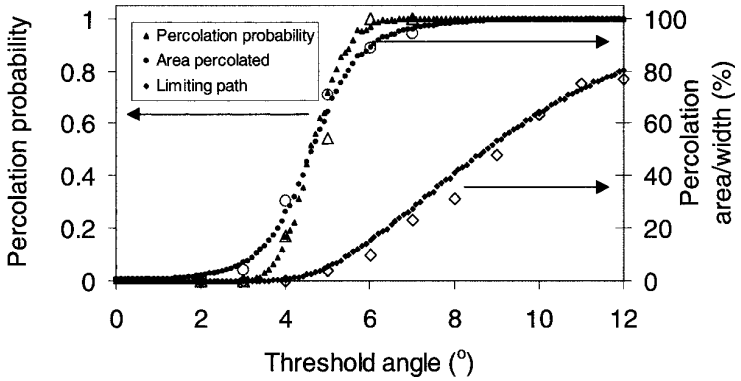

Figure 7. Graph showing the percolation probability, the percolating area and the fraction of the sample width through which flow may occur. In all cases, the modelled data are indicated by the smaller, full symbols and the EBSD data by the larger open symbols.

calculated from EBSD measurements, being dominated by the low-angle misorientations [5]. This dominance has previously been associated with a local correlation of neighbouring grains, because it has a different form from that predicted by bulk texture data, but this need not necessarily be the case. Obviously, the majority of neighbouring pixels will be part of the same grain and, therefore, the measured misorientation of such pixels, as recorded on the histogram, will be determined by the experimental uncertainty in the measurement.

The EBSD data comprise an array of 64 × 48 square pixels and encompass approximately 70 grains. Of the 6032 pixel-to-pixel boundaries examined here, only approximately 18% of them should also be grain boundaries (i.e. lie at the edge of a grain). The model results (for inter-grain boundaries) are shown as the dotted bars on figure 6. The misorientations of many sets of adjacent grains were calculated, then normalized to represent approximately 1000 boundaries. Note that nowhere in the model is any grain-to-grain correlation assumed, the grain orientations are determined solely by bulk texture data.

The fit between the two sets of data is excellent except for the first couple of degrees, which can be explained fully by the resolution of the EBSD measurements. The histograms demonstrate that the most common grain boundary angle is around 5° and that there are a significant number of grains misoriented by more than 8°, hence the restrictions noted earlier from figure 5(e).

3.3. Percolation modelling

A region with the same dimensions as that in which EBSD measurements were carried out in figure 5 has been modelled. Using a hexagonal array of 8 rows and 9 columns, as defined previously, a number of percolation parameters may be calculated. This can then be compared with the measured EBSD data, by analysing figures 4 and 5. For any tolerance angle, the parameters described earlier have been determined, that is percolation probability, minimum percolation width and percolation area. These are plotted in figure 7 alongside modelled data. Note that the modelled data are averaged over many such samples. There is a good fit for all three curves, justifying the applicability of the hexagonal grain model used in this situation. The results amplify the point that the width of the limiting path does not rise steeply with angle, as is the case with the other parameters. If we define a critical threshold angle as that at which over 90% of the sample percolates and over 75% of the area is connected, that value in this tape is 5.6°. However, at that angle the width of the narrowest constriction is, on average, just 11% of the total sample width, and so this definition of critical angle is in no way a representation of unimpeded flow through the sample.

3.4. Critical current model

Figure 8 shows how the critical current density would depend on the grain size using the limiting interface model with a two-dimensional array of hexagonal grains. Note that this is equivalent to an analysis of the effect of varying the sample dimensions for a given grain size. The critical current density has been normalized to J_{c0}, which is the value of J_c predicted when all the grain boundary angles are zero (i.e. a single crystal). Figure 8 shows how the model predicts J_c to vary with grain size in three tapes with different aspect ratios. Whilst the performance of such conductors is very much the same for a small grain size (less than about 20 μm in the tapes considered), the difference becomes increasingly marked as the grain size approaches the sample dimensions. If the sample has width greater than its length, then the model predicts that it is favourable to have just a few very large grains in order to obtain a large J_c. However, it should be noted that when very few grains (and thus few grain boundaries) are involved, there will be a much greater variation in the J_c of different samples. Although the average is higher, there will be many more samples with a very low J_c than is the case when the grain size is small. This is shown in the inset of figure 8, which demonstrates the variation in J_c between samples as a function of grain size. More commonly, coated conductors will have $l \gg w$, corresponding to the lower curve of figure 8(a). This indicates that the average J_c increases for a smaller grain size (or larger sample). Therefore, in this case, both high J_c and high uniformity of J_c are favoured for a small grain size. This has significant consequences for coated conductor development.

Figure 9(a) demonstrates how J_c will be affected by altering the width whilst keeping the length and grain size constant. Narrow samples (a few grains wide) can have very low critical current densities but with increasing width, J_c

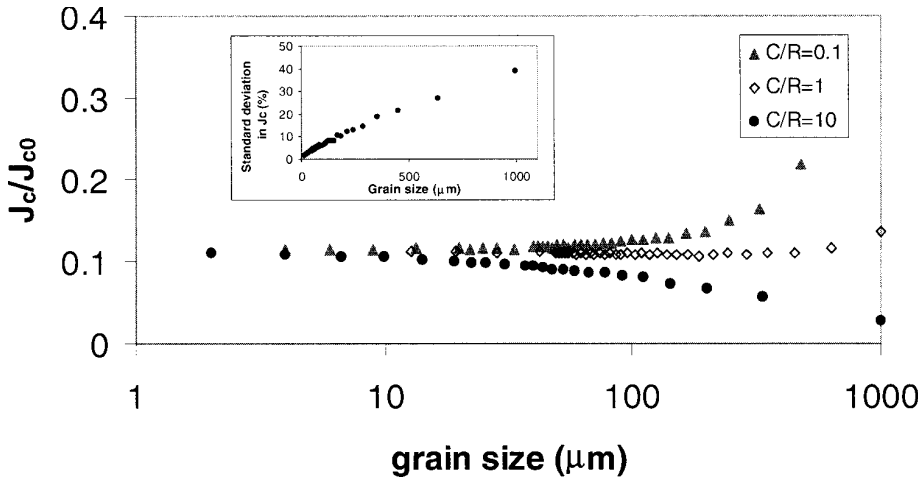

Figure 8. The dependence of J_c on grain size for samples with various aspect ratios and (inset) how the consistency of J_c between samples depends on the grain size.

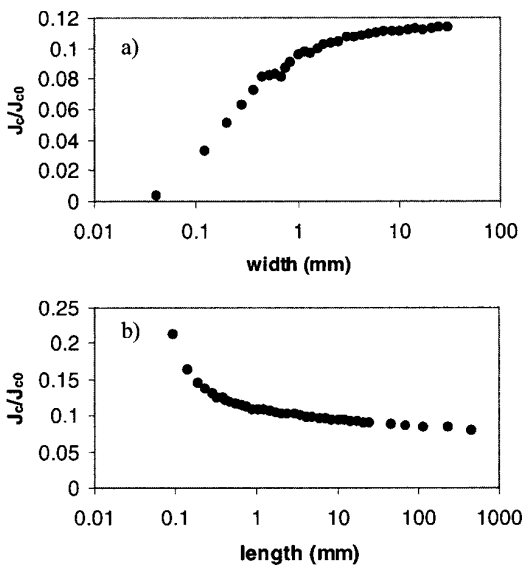

Figure 9. The variation of J_c with (a) sample width and (b) sample length.

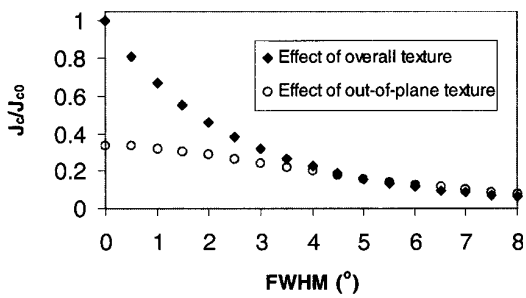

Figure 10. The dependence of J_c on texture. Full triangles show the effect of varying the overall texture. Open circles demonstrate the effect of varying the out-of-plane texture only for a fixed in-plane FWHM of 5°.

increases as there are many more possible percolation paths through the sample. This effect begins to saturate at a value close to 10% of the intragrain J_c. The significance of this result is that from a percolation point of view it would be better to manufacture a single wide tape than to use several narrower ones in parallel.

Figure 9(b) shows the dependence on sample length. As the sample becomes longer, J_c decreases (approximately exponentially for $l \gg w$). This is to be expected as a 10 m long sample can be considered as ten 1 m samples, with the 'worst' of these small lengths determining the J_c of the long conductor. Therefore, when there is less deviation between samples (i.e. small grain size), the length dependence will be weaker. Measurements of the critical currents of long BSCCO high-T_c conductors shows qualitatively the same exponential decrease with increasing length.

All the results so far are based on achieving a crystallographic texture in the superconductor which is exactly the same as that of a given metallic substrate. However, as mentioned earlier, the degree of alignment may well be improved (or indeed may deteriorate) in subsequent layers, and so it is useful to investigate what effect this is likely to have on the current-carrying capacity, figure 10. The full symbols indicate the J_c predicted by the model as one varies the in-plane and out-of-plane alignment together. The open circles show the effect of changing the degree of out-of-plane alignment, whilst maintaining an in-plane FWHM of 5°. It can be seen that having near perfect out-of-plane texture, as may be achieved due to the anisotropic growth mode of YBCO, does not gain such a large advantage in performance.

The model presented here examines how the current-carrying capacity of a coated conductor is affected by bulk texture. There are several other factors which might be considered in order to build up a more complete picture of the limitations on J_c. Grain boundaries which are transferred from the substrate may also cause problems by creating grooves over which the superconductor must be deposited. It is an aim of buffer layer development to ensure that these grooves are covered in order to create a more even surface for deposition. Another problem which has been encountered is that of buffer layer cracking, which can lead to oxygen diffusion through to the substrate. Of course another major factor which determines the overall critical current is the intrinsic quality of the superconducting film.

The best properties have so far been obtained by pulsed laser deposition, although there has been much research into faster, more scalable techniques such as liquid phase epitaxy.

4. Conclusions

The hexagonal grain model and grain-to-grain misorientation histogram both demonstrate a correlation between bulk surface x-ray and grain-to-grain EBSD, with no evidence of grain-to-grain correlation in the NiFe substrate material. The presentation of grain maps with the boundaries marked demonstrates that, even though a percolation path seems apparent, there may be significant obstructions to current flow across a sample.

It will generally be favourable to have a small grain size in order to have high J_c and maintain sample consistency. If one were to produce a sample with a small aspect ratio, however, having just a few large grains would be likely to give a higher critical current. Modelling of the dependence of J_c on width and length shows that, as expected, high critical content densities are obtained in short, wide samples.

Acknowledgments

This work was supported by a grant from the Engineering and Physical Sciences Research Council and was carried out within the framework of the Brite Euram project MUST (BRPR-CT97-0331). EBSD measurements were performed by Oxford Instruments plc.

References

[1] Dimos D, Chaudhari P, Mannhart J and LeGoues F K 1988 *Phys. Rev. Lett.* **61** 219
[2] Verebelyi D T, Feenstra R, Goyal A, Christen D K, Prouteau C, Arendt P N, DePaula R F and Groves J R 1999 *Proc. 9th Int. Workshop on Critical Currents* p 51
[3] Norton D P *et al* 1996 *Science* **274** 755
[4] Prouteau C, Duscher G, Christen D K, Browning N D, Pennycook S J, Chisholm M F, Norton D P, Goyal A and Park C 1997 *Advances in Superconductivity X. Proc. 10th Int. Symp. on Superconductivity* p 1015
[5] Goyal A, Ren S X, Specht E D, Kroeger D M, Feenstra R, Norton D P, Paranthaman M, Lee D F and Christen D K 1999 *Micron* **30** 463
[6] Norton D P *et al* 1998 *Mater. Sci. Eng.* B **56** 86
[7] Park C, Norton D P, Budai J D, Christen D K, Verebelyi D, Feenstra R, Lee D F, Goyal A, Kroeger D M and Paranthaman M 1998 *Appl. Phys. Lett.* **73** 1904
[8] Rhyner J and Blatter G 1989 *Phys. Rev.* B **40** 829
[9] Blatter G, Rhyner J and Dersch H 1989 *Physica* C **162** 355
[10] Evetts J E, Hogg M J, Glowacki B A, Rutter N A and Tsaneva V N 1999 *Supercond. Sci. Technol.* **12** 1050
[11] `www.Oxford-Instruments.com/mag/index.cfm`
[12] Mulet R, Diaz O and Altshuler E 1997 *Supercond. Sci. Technol.* **10** 758
[13] Bunge H J 1982 *Texture Analysis in Materials Science* (London: Butterworths) p 4
[14] Goyal A, Specht E D, Kroeger D M and Mason T A 1996 *Appl. Phys. Lett.* **68** 711